Available online at www.sciencedirect.com

ScienceDirect

Procedia Engineering 160 (2016) 151 – 157

Procedia Engineering

www.elsevier.com/locate/procedia

XVIII International Colloquium on Mechanical Fatigue of Metals (ICMFM XVIII)

Ultra-slow fatigue crack propagation in metallic alloys

C. Sarrazin-Baudoux[a], S.E. Stanzl-Tschegg[b]*, B.M. Schönbauer[b], J. Petit[a]

[a]*Pprime Institute, UPR CNRS 3346, Dept. of Physics and Mechanics of Materials, ENSMA, Chasseneuil-Futuroscope, France*
[b]*University of Natural Resources and Life Sciences, Vienna (BOKU), Institute of Physics and Materials Science, Vienna, Austria*

Abstract

The influence of frequency (20 kHz ultrasonic tests and conventional 20 to 35 Hz tests) and environment (air and vacuum) on near-threshold fatigue crack propagation of three metallic alloys, Ti-6Al-4V, 2024-T351 and 12% Cr stainless steel is compared experimentally. The effective stress-intensity factor which is considered as the propagation driving force is determined from closure measurements or tests run at high *R*-ratio. Based on microfractographic observations, the results are discussed in terms of a preexisting model for intrinsic and environmentally assisted fatigue crack propagation.

Peer-review under responsibility of the University of Oviedo

Keywords: metallic alloys; fatigue crack propagation; ultrasonic fatigue; thresholds, air humidity.

1. Introduction

During in-service loading, turbine-engine components of airplanes experience high frequency vibration loads (~ 1 to 2 kHz) due to resonant airflow dynamics which are often superimposed to a high mean stress. Because of the high frequencies, even cracks growing at ultraslow velocities (< 10^{-10} m/cycle) can lead to failure of a component. Consequently, it is of prime importance to know the fatigue crack propagation behavior and, moreover, the threshold-stress intensity factor for fatigue cracks at very high frequency. This paper is dedicated to a comparative study of fatigue crack propagation in the near threshold domain at a conventional frequency of 20-35 Hz and at ultrasonic frequency of 20 kHz in air and in vacuum for three alloys: Ti-6Al-4V alloy (TA6V) used for disks of turbine engines, 2024-T351 aluminum alloy for airplane structures and 12% Cr martensitic stainless steel AISI403

* Corresponding author. Tel.: +43-1-47654-89260; fax: +43-1-47654-89259.
E-mail address: stefanie.tschegg@boku.ac.at

Peer-review under responsibility of the University of Oviedo
doi:10.1016/j.proeng.2016.08.875

used for turbine blades. The influence of atmosphere environment is examined by tests performed in ambient air and in high vacuum. The results are discussed on the basis of an existing model for ambient-air assisted fatigue crack propagation in metallic alloys.

2. Experimental

Three different alloys were studied:

i) bimodal Ti-6Al-4V plates in overaged condition (1h at 925°C and 2h at 700°C) with approx. 60% primary α phase and 40% lamellar α+β colonies. The static properties are: Ultimate tensile strength, R_m = 970 MPa, Yield strength, $R_{p0.2}$ = 930 MPa, Fracture toughness, K_{IC} = 67 MPa√m and Young´s modulus, E = 116 GPa;
ii) 2024-T351 Al in underaged condition with a pancake microstructure and with R_m = 578 MPa, $R_{p0.2}$ = 441 MPa, K_{IC} = 32 MPa√m and E = 70 GPa;
iii) 12% Cr martensitic stainless steel AISI403 hardened at 913°C and tempered at 649°C and 621°C. The mean grain size is 6 µm, and R_m = 799 MPa, $R_{p0.2}$ = 611 MPa and E = 215 GPa.

Tubular specimens with a wall thickness of 2 mm, as shown in Fig. 1(a), were used to perform ultrasonic experiments at positive R-ratios. A drilled hole and a notch were machined for a defined place of crack initiation. Experimental details for the ultrasonic measurements are given in [1]. The specimens were loaded with controlled mean loads which served to realize load ratios at R = 0.05 to R = 0.8. Intermittent loading with periodic pauses between pulses allowed cooling of the specimens in addition to forced-air cooling in tests in ambient air. In servo-hydraulic experiments, standard compact tension (CT) specimens (Fig. 1(b)) with a width of 40 mm and a thickness of 8 mm were used. In order to compare servo-hydraulic and ultrasonic fatigue tests, similar experimental load shedding procedures with 5–7% steps to reduce the loads were used after crack length increments of 0.15 to 0.20 mm.

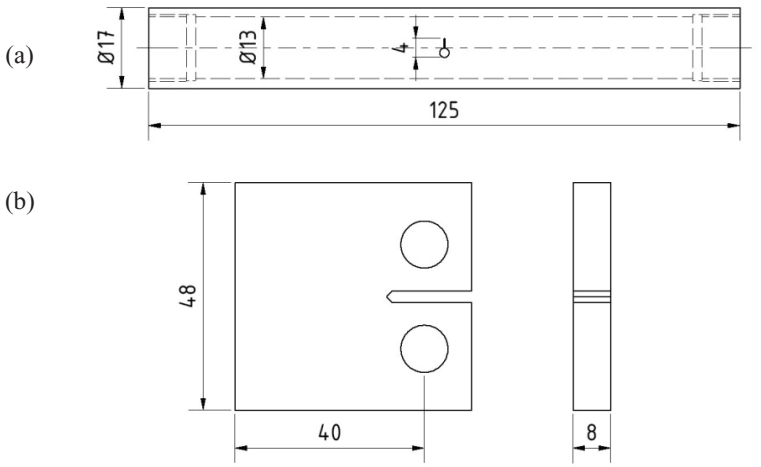

Fig. 1. (a) Tubular specimen for 20 kHz ultrasonic experiments; (b) CT specimen used for servo-hydraulic experiments (dimensions in mm).

3. Experimental results

3.1. Influence of R-ratio, test frequency and environment on fatigue crack propagation in TA6V

The fatigue crack-growth rates d*a*/d*N* versus the stress intensity factor range Δ*K* are presented in Fig. 2(a) for tests at three different *R*-ratios on Ti-6Al-4V at 20 kHz [2]. As classically observed, increasing *R*-ratios result in accelerated d*a*/d*N* values and lower threshold ranges. Fig. 2(b) shows crack growth data obtained on this alloy at $R = 0.8$ at 35 Hz and 20 kHz and data obtained previously on another bimodal TA6V alloy [4]. All data fall within the same scatter band and confirm the same behavior of this alloy.

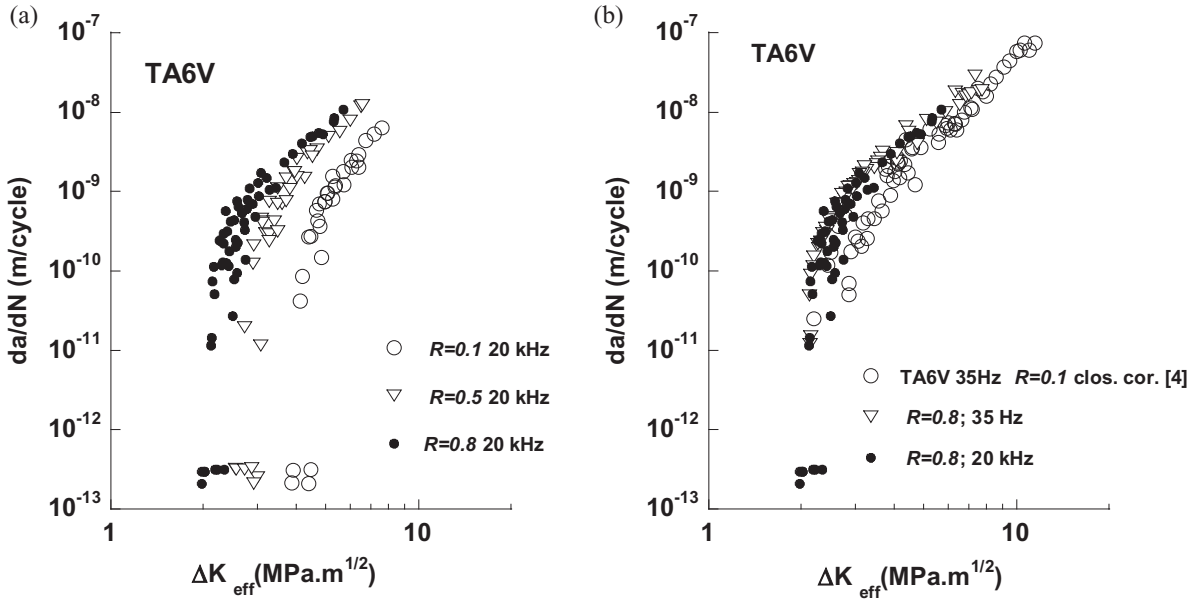

Fig. 2. (a) Influence of *R*-ratio on fatigue-crack propagation rates in bimodal TA6V in air at 20 kHz [2]; (b) comparison of closure corrected $R = 0.8$ data in air of bimodal TA6V at 20 kHz and 20 Hz data of bimodal TA6V [4].

In Fig. 3(a), data of high-vacuum tests on the presently studied bimodal alloy at 1 kHz and $R = 0.6$ [5] are plotted in comparison with the present data at $R = 0.8$ and effective data (closure corrected) on TA6V in air and in high vacuum (~10^{-4} Pa) at $R = 0.1$ [4]. No influence of frequency on the propagation rate d*a*/d*N* and on the threshold range in vacuum as well as in ambient air can be recognized. The effective data on TA6V resulting from [4] are in accordance with data at $R = 0.6$ of the present alloy. Hence all data can be considered as effective data. These results exhibit a huge effect of atmosphere environment on crack growth rates in air which are about two to three orders of magnitude higher than in vacuum. The influence of air environment on the threshold is more difficult to interpret due to the large scatter of the measurements in high vacuum at high frequency.

Based on the two-step framework modeling proposed by Petit et al. [6] and Sarrazin-Baudoux et al. [7], the acceleration of the propagation in air can be explained with a detrimental effect of the atmospheric water vapor. The first step of the phenomenon is a reduction of the energy required to create a new surface induced by water vapor adsorption at the crack tip (Fig. 3(a): regime IIad). The second step is, in some critical conditions, hydrogen assistance (Fig. 3(a): regime IIhyd) by hydrogen atoms resulting from the dissociation of adsorbed water vapor molecules [6]. The highly retarded propagation in high vacuum is analyzed as a combination of the effect of absence of environment assistance and of the effect of localization of the deformation within the basal slip planes [6,7] leading to a very rough crystallographic crack path when slip reversibility corresponds to the stage I-like regime compared to the intrinsic stage II (Fig. 3(a): regime IIint) which prevails at mid Δ*K* values [6]. The crystallographic

propagation in vacuum (Fig. 3(c)), corresponds to the highly retarded intrinsic stage I-like regime (Fig. 3(a): St. I-like) [4,5] and the stage II propagation in air, with a flat crack path normal to the load axis, as illustrated in Fig. 3(b).

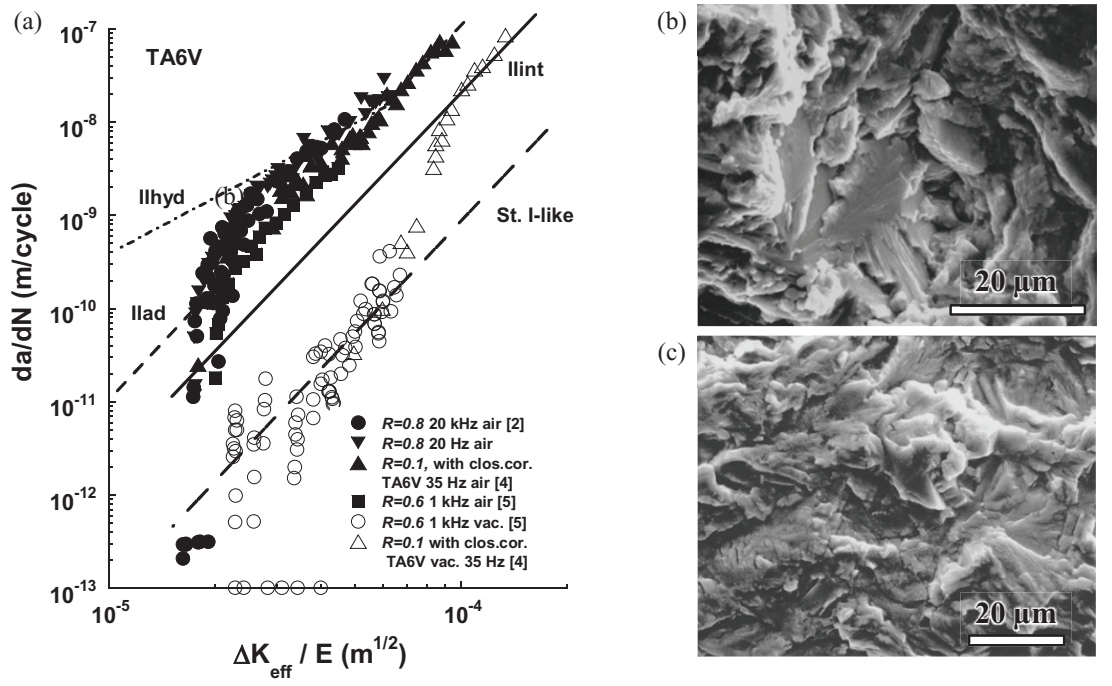

Fig. 3. (a) Influence of environment and frequency on crack propagation in Ti-6Al-4V alloy; (b) stage II crack path at 1 kHz, $R = 0.6$ in air; c) crystallographic crack path at 1 kHz, $R = 0.6$ in vacuum.

3.2. Influence of environment and test frequency in 2024-T351 alloy

In Fig. 4(a), data on a 2024-T351 alloy are plotted that were obtained in air and in vacuum at conventional frequency (20 Hz) and ultrasonic frequency (20 kHz) in comparison to other 2024-T351 specimens tested at 35 Hz [8]. The diagram da/dN versus $\Delta K/E$ and $\Delta K_{eff}/E$ shows that at $R = 0.5$ the rates measured above 3×10^{-9} m/cycle seem poorly affected by crack closure and test frequency. But in the near-threshold domain, the contribution of crack closure becomes substantial showing that, data at $R = 0.5$ are no more representative of effective data. It is assumed that, data at $R = 0.8$ give a better approach of the effective behavior for TA6V. However, whatever the frequency, the influence of environment is very large for da/dN lower than 10^{-8} m/cycle and is similar at all frequencies.

In the 2024-T351 alloy, the near-threshold crack path in vacuum becomes highly crystallographic leading to very slow rates and corresponds to the stage I-like intrinsic propagation as previously identified [6,8]. The fracture-surface morphology illustrated in Figs. 4(b) and 4(c) shows a huge change in the mechanism when the propagation switches from stage II to stage I-like at 35 Hz as well as 20 kHz. This transition occurs between 10^{-8} and 10^{-9} m/cycle as pointed out above for the Ti alloy.

3.3. Influence of environment and test frequency on 12% Cr martensitic stainless AISI403 steel

The da/dN vs ΔK diagrams for tests performed in air and in high vacuum on the AISI403 steel at 20 kHz at high load ratio $R = 0.8$ [10] are presented in Fig. 5(a) in comparison with a previous test run in air at 35 Hz on a similar

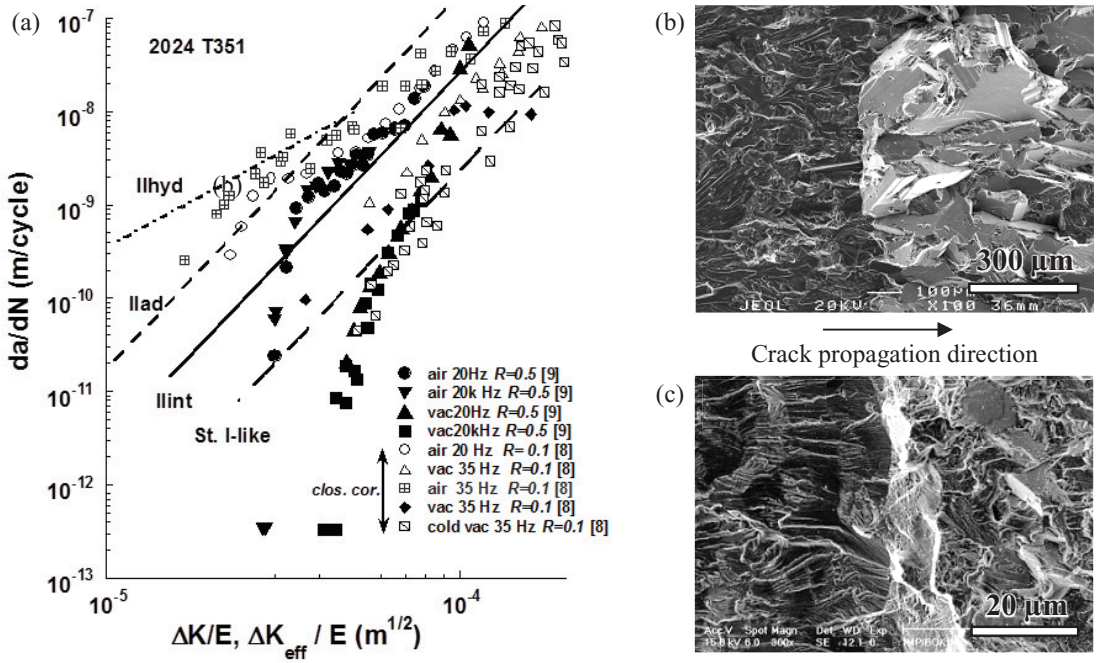

Fig. 4. (a) Influence of environment and frequency on fatigue-crack propagation in 2024-T351 alloy; (b) cold air- vacuum transition in 2024-T351 at 35 Hz [8] and (c) air-vacuum transition near threshold in 2024-T351 at 20 kHz [9] .

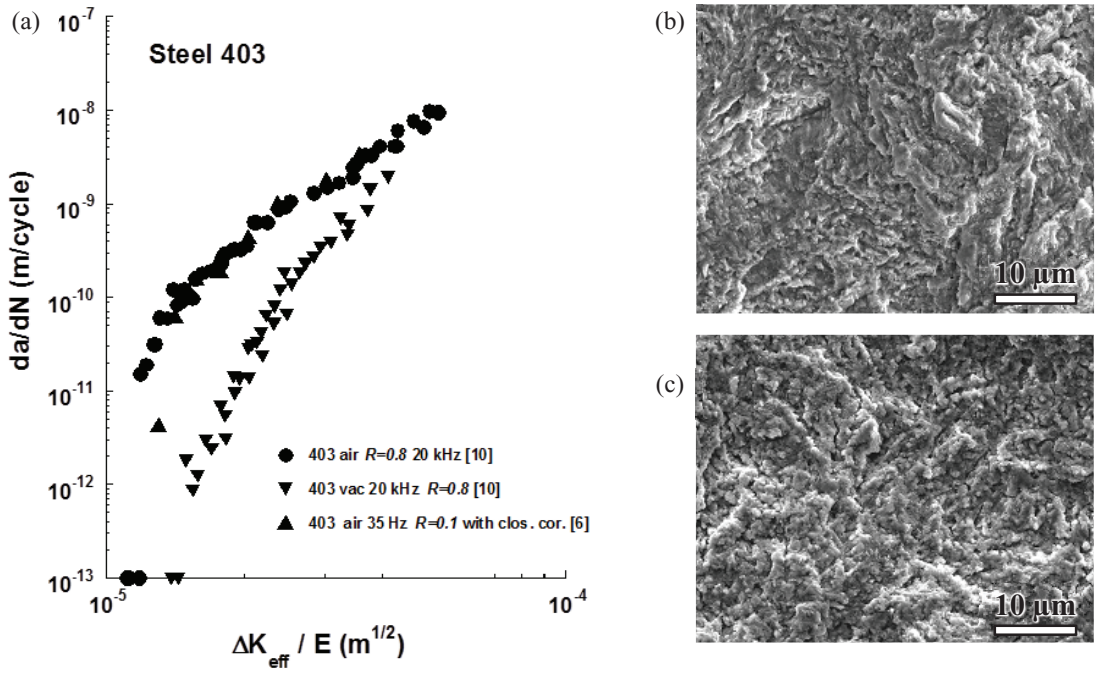

Fig. 5. (a) Influence of environment and test frequency on AISI403 steel [10,6]; (b) near threshold fracture surface in air at 20 kHz [10]; (c) near threshold fracture surface in vacuum at 20 kHz [10].

alloy with closure correction [6]. Similar to the TA6V alloy, it is clearly shown that data at $R = 0.8$ are consistent with the effective data and confirm the absence of crack closure contribution for such loading condition. A substantial effect of environment is observed on the effective threshold level and on da/dN in all the explored ranges. The ultraslow fracture-surface morphology at 20 kHz is illustrated in Figs. 5(b) for air and in 5(c) for high vacuum without detectable effect of environment on the associated mechanism

4. Analysis of results

Slip localization on basal plane in Ti alloy [7] and (111) planes in the overaged 2024-T351 alloy containing shearable precipitates [6,8] are the main characteristics of the intrinsic propagation in both alloys, inducing a crystallographic stage I-like regime so that the crack-growth rates are strongly lowered by boundary barriers, crack branching and deviation in comparison to the more conventional stage II propagation which is poorly sensitive to the microstructure. The different regimes are shown in accordance with the framework modeling proposed by Petit et al [6].

In Fig. 6(a), da/dN vs $\Delta K/E$ diagrams are plotted to account for the difference in Young's modulus for the two base metals, i.e. Al and Ti. A remarkable similitude is observed for TA6V and 2024-T351 alloy with, for both alloys, a huge detrimental effect of water vapor and of the localization of deformation at low ΔK within individual grains along the crack front favored by microstructures promoting basal plane slip. In Fig. 6(b), the behavior of the AISI403 steel at 20 kHz and $R = 0.8$ is shown to be consistent with the effective behavior of different other steels [6] independent of the frequency. In both, air and vacuum, the propagation is in accordance with the intrinsic stage II in vacuum, and a stage II assisted by water vapor in air.

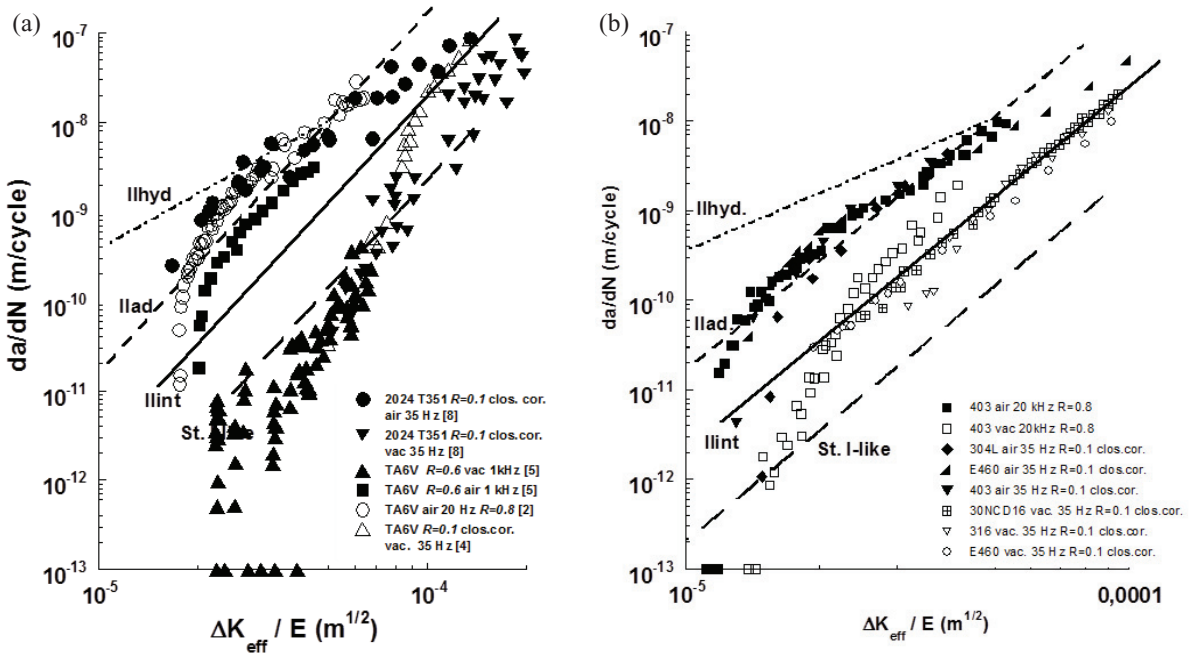

Fig. 6. (a) (a) Comparison of da/dN vs $\Delta K_{eff}/E$ data for TA6V and 2024-T351; (b) comparison of da/dN vs ΔK/E data for AISI403 steel at 20 kHz [10] and $R = 0.8$ to da/dN vs $\Delta K_{eff}/E$ for different steels at 35 Hz [6].

5. Conclusions

From the present study on ultraslow fatigue crack propagation in a selection of metallic alloys, the following conclusions can be drawn:

- The influence of ambient-air environment is comparable at 20 kHz and conventional frequencies of 20-35 Hz;
- Data at $R = 0.8$ - whatever the frequency is - are comparable to that obtained after correction for crack closure and thus correspond to the effective behavior of the alloys, i.e. da/dN vs ΔK_{eff}.
- In ambient air, the decrease of the resistance to fatigue crack growth can be attributed to a detrimental effect of water vapor resulting in a corrosion-assisted stage II mode in all the alloys.
- In high vacuum, ultraslow crystallographic fatigue crack propagation is identified as a stage I-like regime in TA6V and 2024-T351 alloys which favors a localization of deformation within the crack tip. In the AISI403 steel, an intrinsic stage II regime prevails similar as in some other steels.
- All the crack growth rate data expressed in terms of the effective stress intensity factor range ΔK_{eff} are conveniently described using an existing framework model for intrinsic and environmentally assisted propagation regimes.

References

[1] S.E. Stanzl-Tschegg, Ultrasonic Fatigue, Keynote, Proc. 6th Int. Fatigue Congress, Berlin, Elsevier Sci. Ltd. III, 1996, pp. 1887-1898.
[2] C. Sarrazin-Baudoux, S.E. Stanzl-Tschegg, H. Mayer, J. Petit, Ultra slow crack propagation in TA6V Titanium alloy, VHCF 5, June 2011, Berlin, pp.133-138.
[3] W. Elber, Fatigue crack closure under cyclic tension, Eng Fract Mech 2(1), 1970, pp. 37-45.
[4] W. Berata, Résistance à la fissuration en fatigue à temperature élevée de l'alliage TA6V, PhD thesis, University of Poitiers, France, 1992.
[5] R.O. Ritchie, D.L. Davidson, B.L. Boyce, J.P. Campbell, O. Roder, High-cycle fatigue in Ti-6Al-4V, Fatigue Fract Eng M 22, 1999, pp. 621-631.
[6] J. Petit, G. Henaff and C. Sarrazin-Baudoux, Environmentally assisted fatigue in the gaseous atmosphere, in: Petit J, Scott P, (Eds.), Comprehensive Structural Integrity, Vol. 6, Elsevier Pub., Oxford, UK, 2003, pp.211-280.
[7] C. Sarrazin, R. Chiron, S. Lesterlin, J. Petit, Electron backscattering pattern identification of surface morphology of fatigue cracks in TA6V, Fatigue Fract Eng M, 17(12), 1994, pp.1383-1389.
[8] C. Gasqueres, Fissuration par fatigueet ténacité d'alliages d'aluminium 2xxx à 223K, PhD thesis, University of Poitiers, France, 2002.
[9] B. Holper, H. Mayer, A.K. Vasudevan, S.E. Stanzl-Tschegg, Near threshold fatigue crack growth in aluminium alloys at low and ultrasonic frequency: Influences of specimen thickness, strain rate, slip behaviour and air humidity, Int J Fatigue, 25, 2003, pp. 397-411.
[10] B. M. Schönbauer, S.E. Stanzl-Tschegg, Influence of environment on the fatigue crack growth behaviour of 12% Cr steel, Ultrasonics 53, 2013, pp. 1399-1405.